Springer

KSME

Journal of Mechanical Science and Technology 32 (7) (2018) 2973~2985
www.springerlink.com/content/1738-494x(Print)/1976-3824(Online)
DOI 10.1007/s12206-018-0601-2

Adaptive control of a vehicle-seat-human coupled model using quasi-zero-stiffness vibration isolator as seat suspension†

Yong Wang[1,*], Shunming Li[2], Chun Cheng[3] and Yuqing Su[4]

[1]*Automotive Engineering Research Institute, Jiangsu University, Zhenjiang 212013, China*
[2]*College of Energy and Power Engineering, Nanjing University of Aeronautics and Astronautics, Nanjing 210016, China*
[3]*School of Mechatronic Engineering, Jiangsu Normal University, Xuzhou 221116, China*
[4]*Advanced Vehicle Development & Vehicle Intergration, Pan Asia Technical Automotive Center Co., Ltd., Shanghai 201201, China*

(Manuscript Received September 25, 2015; Revised March 14, 2018; Accepted March 20, 2018)

Abstract

We propose the quasi-zero-stiffness (QZS) vibration isolator as seat suspension to improve vehicle vibration isolation performance. The QZS vibration isolator is composed of vertical spring and two symmetric negative stiffness structures used as stiffness correctors. A vehicle-seat-human coupled model considering the QZS vibration isolator is established as a three degree-of-freedom (DOF) model; it is composed of a quarter car model and a simplified 1 DOF model combined vehicle seat and human body. This model considers the changing mass of the passengers and sets the total mass of the vehicle seat and human body as an uncertain parameter, which investigates the overload and unload conditions in practical engineering. To further improve the vehicle ride comfort, a constrained adaptive back-stepping controller law based on the barrier Lyapunov function (BLF) is presented. The dynamic characteristic of the active vehicle-seat-human coupled model under shock excitation was analyzed using numerical method. The results show that the designed controller law can isolate the shock excitation transmitted from the road to the passengers effectively, and both the vehicle and seat suspension strokes remain in the allowed stroke range.

Keywords: Adaptive control; Quasi-zero-stiffness; Seat suspension; Vehicle-seat-human coupled model; Vibration isolator

1. Introduction

In practical engineering, a low frequency vibration seriously affects human health and reduces working efficiency. Seat suspension can be used to attenuate high amplitude vibration transmitted from the road to the passengers in low frequency range and improve vehicle ride comfort [1]. As is well known, a linear seat suspension can provide an effective isolation when the excitation frequencies are larger than $\sqrt{2}$ -times the natural frequency of the vibration system. Reducing spring stiffness can lead to a wider isolation frequency band, but results in a lower load bearing capacity and a larger static displacement between the seat and the vehicle floor. However, this dilemma can be eliminated by using quasi-zero-stiffness (QZS) vibration isolator [2, 3] as seat suspension. The QZS vibration isolator is composed of a load bearing elastic element providing positive stiffness and special mechanisms providing negative stiffness named as stiffness correctors. The load bearing elastic element is usually the vertical spring; after being loaded at the static equilibrium position, the positive stiffness of the vertical spring is exactly balanced by the negative stiffness provided by the stiffness correctors, then a small dynamic stiffness can be achieved to obtain a lower natural frequency and a wider isolation frequency band. So the QZS vibration isolator can have a high static stiffness with a small static displacement without sacrificing the load bearing capacity and a small dynamic stiffness to achieve a low natural frequency, which is superior to the linear vibration isolator. Many researchers have proposed various different types of stiffness correctors. Carrella et al. [4, 5], Kovacic et al. [6] and Wang et al. [7] considered a QZS vibration isolator by using inclined springs as stiffness correctors and investigated the static and dynamic characteristics theoretically. Robertson et al. [8], Zhou et al. [9] and Xu et al. [10] used electromagnetic or magnetic springs as stiffness correctors to build a QZS vibration isolator and studied the static and dynamic characteristics in detail. Liu et al. [11, 12] designed a QZS vibration isolator by using Euler buckled or sliding beams as stiffness correctors and analyzed the dynamic behavior theoretically. Shaw et al. [13] used a bistable composite plate as stiffness correctors to form a QZS vibration isolator and analyzed the dynamic response theoretically and experimentally. Ahn et al.

*Corresponding author. Tel.: +86 15951897282, Fax.: +86 511 88782845
E-mail address: wangy1921@126.com
† Recommended by Associate Editor Hyoun Jin Kim

[14] designed a QZS vibration isolator by using cam-roller mechanism as stiffness correctors and found the desired QZS characteristics can be achieved with properly designed cam geometry.

Le and Ahn [15] built a QZS vibration isolator composed of a positive stiffness mount and two symmetric negative stiffness structures for improving the vehicle seat isolation performance. They also designed a fuzzy sliding mode controller [16] or an adaptive intelligent back-stepping controller [17] to further improve the performance. In their studies, road excitation is applied to the vehicle floor, which is unsuitable for some practical engineering cases, because road excitation is filtered by vehicle suspension in both amplitude and frequency when transmitted to the vehicle floor [18]. Also, when loading a specific designed mass, the dynamic stiffness of the QZS vibration isolator is considered to be zero at the static equilibrium position, then the QZS characteristic can be obtained; the force-displacement and stiffness-displacement relationships about the static equilibrium position are symmetric. In fact, the static equilibrium position of the QZS vibration isolator is sensitive to the loaded mass; when the QZS vibration isolator loads a mass larger or smaller than the specific designed mass, the system would not be balanced at the original static equilibrium position, and the force-displacement and stiffness-displacement relationships about the new static equilibrium position would be asymmetric. So for the vehicle seat, when the mass of the passengers varies, the actual mass of the passengers can hardly match the specific designed mass, so the QZS vibration isolator would be in the overload or unload conditions. In addition, they neglected to investigate the vehicle and seat suspension strokes, which are two main important factors for the vehicle and seat suspensions design. So here we propose the QZS vibration isolator as seat suspension, consider the overload and unload conditions, and apply road excitation directly to the vehicle wheel, which are more close to the actual conditions.

In the author's previous paper [19], a vehicle-seat-human coupled model considering the QZS vibration isolator is established as a 8 degree-of-freedom (DOF) model that is composed of a quarter car model [20] (2 DOF), a seat suspension model (2 DOF) and a human body model [21] (4 DOF). Although the quarter car model is simple, it can provide qualitatively correct information for vehicle ride comfort studies in low frequency range. The seat suspension model includes two parts-seat frame and seat cushion. The human body model contains four important human body parts--thighs, lower torso, upper torso and head. In this paper, in order to consider the changing mass of the passengers, the vehicle-seat-human coupled model is established as a 3 DOF model that is composed of a quarter car model (2 DOF) and a simplified 1 DOF model combined vehicle seat and human body. The total mass of the vehicle seat and human body is considered as an uncertain parameter, which can investigate the overload and unload conditions.

In Ref. [19], the dynamic characteristic of the vehicle-seat-human coupled model under road shock and random excitations is analyzed using numerical method. The results show that when the QZS vibration isolator is used as seat suspension, the vehicle ride comfort improves effectively compared to the linear seat suspension, and the vehicle and seat suspension strokes remain in the allowed stroke range. When the vehicle-seat-human coupled model subjects to road shock excitation, as the road excitation displacement or the vehicle forward velocity increases, the peak acceleration value of human body increases for both kinds of seat suspensions, so the vehicle ride comfort becomes poorer. Since the vehicle-seat-human coupled model proposed in this paper is an uncertain nonlinear system, and also to further improve the vehicle ride comfort, a constrained adaptive back-stepping controller law [22] based on the barrier Lyapunov function (BLF) [23, 24] is presented. This control law can achieve a good performance when nonlinearity and uncertain parameters exist in the dynamic model.

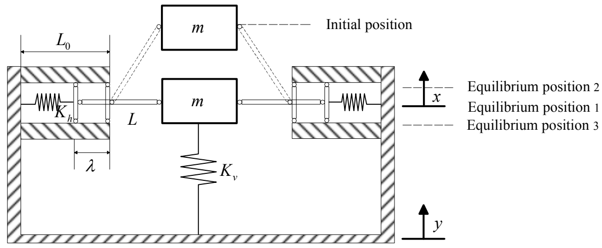

Fig. 1. Scheme of a QZS vibration isolator.

This paper is organized as follows. A QZS vibration isolator is presented and brief description of static analysis is shown in Sec. 2. In Sec. 3, the active vehicle-seat-human coupled model of 3 DOF using QZS vibration isolator as seat suspension is established. The constrained adaptive back-stepping controller law is presented in Sec. 4. In Sec. 5, the dynamic characteristic of this active vehicle-seat-human coupled model subject to shock excitation is obtained using numerical method, and the usefulness of the controller law is addressed. In Sec. 6, the comparison of the control effect for the active model with QZS and linear vibration isolators used as seat suspensions is discussed. Sec. 7 concludes the paper.

2. QZS vibration isolator model

A QZS vibration isolator composed of vertical spring and two symmetric negative stiffness structures used as stiffness correctors is shown in Fig. 1. This model has been studied in detail in Ref. [25], so only brief description is presented here.

Fig. 1 shows when loading a mass m, the system is balanced at the static equilibrium position-equilibrium position 1. The stiffness of the vertical and horizontal springs is K_v and K_h; the initial length of the horizontal springs is L_0; the compression deformation of the horizontal springs when the system at the static equilibrium position is λ; the length of the connecting element is L; x is the displacement of the mass from the

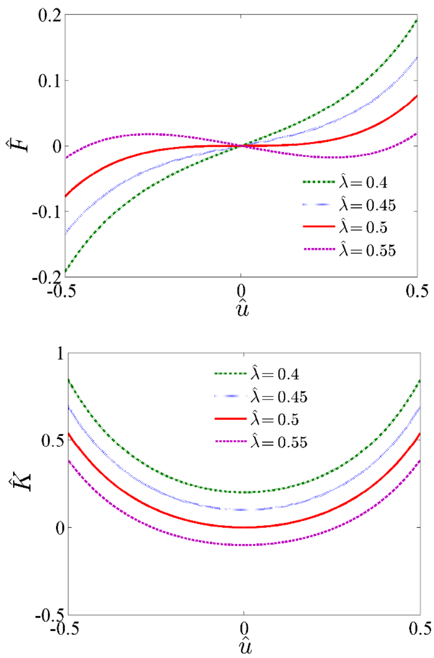

Fig. 2. Non-dimensional force-displacement and stiffness-displacement curves.

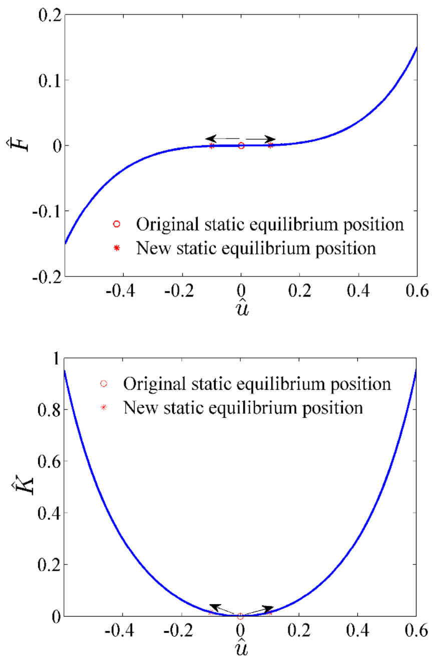

Fig. 3. Original and new equilibrium positions of the QZS vibration isolator.

static equilibrium position and y is the displacement of the base excitation. The force-displacement and stiffness-displacement relationships of the system are given as

$$\begin{cases} F = K_v u - 2K_h\left[\lambda - \left(L - \sqrt{L^2 - u^2}\right)\right]\dfrac{u}{\sqrt{L^2 - u^2}} \\ K = \left(K_v - 2K_h\right) + \dfrac{2K_h\left(L-\lambda\right)L^2}{\left(L^2 - u^2\right)^{\frac{3}{2}}} \end{cases} \tag{1}$$

where $u = x - y$. Eq. (1) can be written in non-dimensional form as

$$\begin{cases} \hat{F} = \left(1-2k\right)\hat{u} + 2k\left(1-\hat{\lambda}\right)\dfrac{\hat{u}}{\sqrt{1-\hat{u}^2}} \\ \hat{K} = \left(1-2k\right) + \dfrac{2k\left(1-\hat{\lambda}\right)}{\left(1-\hat{u}^2\right)^{\frac{3}{2}}} \end{cases} \tag{2}$$

where $\hat{u} = u/L$, $\hat{\lambda} = \lambda/L$, $k = K_h/K_v$, $\hat{F} = F/\left(K_v L\right)$, $\hat{K} = K/K_v$.

If the stiffness of the QZS vibration isolator is zero at the static equilibrium position, the QZS characteristic can be obtained, then $\hat{\lambda}_{qzs} = 1/\left(2k\right)$.

The non-dimensional force-displacement and stiffness-displacement curves of the QZS vibration isolator for various values of $\hat{\lambda}$ when $k = 1$ are shown in Fig. 2. It can be clearly seen that if $\hat{\lambda} = \hat{\lambda}_{qzs}$, the positive stiffness of the vertical spring is balanced by the negative stiffness provided by the stiffness correctors at the static equilibrium position, so the QZS characteristic can be achieved. If $\hat{\lambda} > \hat{\lambda}_{qzs}$, the stiffness is negative in the neighborhood of the static equilibrium position, then the system can be unstable, which is an undesirable condition. When $\hat{\lambda} < \hat{\lambda}_{qzs}$, the stiffness of the QZS vibration isolator maintains a small positive value at the static equilibrium position. So to keep the stiffness positive, $\hat{\lambda}$ should be smaller than or equal to $\hat{\lambda}_{qzs}$. In this study, the case $\hat{\lambda} \le \hat{\lambda}_{qzs}$ was considered.

If the QZS vibration isolator is loaded with a mass smaller or larger than the specific designed mass, the mass will not load the QZS vibration isolator statically to its minimum tangent stiffness position at the original static equilibrium position-equilibrium position 1, the QZS vibration isolator is in the unload or overload conditions, and the new static equilibrium position would be equilibrium position 2 or equilibrium position 3. The force-displacement and stiffness-displacement relationships about this new static equilibrium position would be asymmetric, as can be clearly seen in Fig. 3.

3. Active vehicle-seat-human coupled model

The active vehicle-seat-human coupled model of 3 DOF using QZS vibration isolator as seat suspension is shown in Fig. 4; it is composed of a quarter car model (2 DOF) and a simplified 1 DOF model combined vehicle seat and human body: m_1 is the mass of wheel, m_2 is the mass of vehicle body, m_{31} and m_{32} are the masses of the vehicle seat and human body, respectively, and $m_3 = m_{31} + m_{32}$; c_1, c_2 and k_1, k_2 are the damping and stiffness of the wheel and vehicle body, respectively; c_3 is the damping of the vehicle seat, and F_{s3} is the spring force of the vehicle seat; $z_{1\sim3}$ are the displace-

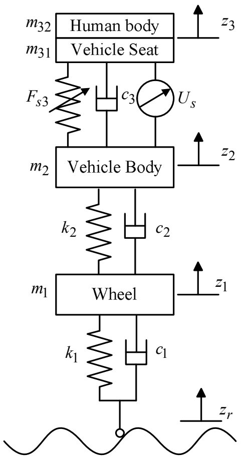

Fig. 4. Active vehicle-seat-human coupled model.

ments of the corresponding masses, z_r is the road excitation displacement and is applied directly to the vehicle wheel; U_s is the active input of the seat suspension system.

Denote m_{s3} as the specific designed mass of the vehicle seat and human body, when $m_3 = m_{s3}$, the dynamic equations of the active vehicle-seat-human coupled model in the corresponding static equilibrium positions of the masses are given by

$$\begin{cases} m_1\ddot{z}_1 = c_2\left(\dot{z}_2 - \dot{z}_1\right) + k_2\left(z_2 - z_1\right) \\ \qquad -c_1\left(\dot{z}_1 - \dot{z}_r\right) - k_1\left(z_1 - z_r\right) \\ m_2\ddot{z}_2 = c_3\left(\dot{z}_3 - \dot{z}_2\right) + F_{s3} - c_2\left(\dot{z}_2 - \dot{z}_1\right) \\ \qquad -k_2\left(z_2 - z_1\right) - U_s\left(t\right) \\ m_3\ddot{z}_3 = -c_3\left(\dot{z}_3 - \dot{z}_2\right) - F_{s3} + U_s\left(t\right). \end{cases} \tag{3}$$

When the QZS and linear vibration isolators are used as seat suspension respectively, F_{s3} can be obtained as

$$\begin{cases} F_{s3} = K_v\left(1-2k\right)\left(z_3 - z_2\right) \\ \qquad +2kK_vL(1-\hat{\lambda})\dfrac{\left(z_3 - z_2\right)}{\sqrt{L^2 - \left(z_3 - z_2\right)^2}} \\ F_{s3} = K_v\left(z_3 - z_2\right) \end{cases} \tag{4}$$

where K_v is the stiffness of linear seat suspension. In this case, the mass m_3 loads the QZS vibration isolator statically to its minimum tangent stiffness position at the static equilibrium position; the force-displacement and stiffness-displacement relationships about the static equilibrium position are symmetric, which can be clearly seen in Figs. 1 and 3. When m_3 is larger or smaller than the specific designed mass m_{s3}, the seat suspension system will not be balanced at the original static equilibrium position, F_{s3} can be given in a general form, Eq. (4) can be written as

$$\begin{cases} F_{s3} = K_v\left(1-2k\right)\left(z_3 - z_2 + u_n\right) - \left(m_3 - m_{s3}\right)g \\ \qquad +2kK_vL(1-\hat{\lambda})\dfrac{\left(z_3 - z_2 + u_n\right)}{\sqrt{L^2 - \left(z_3 - z_2 + u_n\right)^2}} \\ F_{s3} = K_v\left(z_3 - z_2 + u_n\right) - \left(m_3 - m_{s3}\right)g \end{cases} \tag{5}$$

where u_n is the new static equilibrium position. When $m_3 = m_{s3}$, $u_n = 0$; when $m_3 \neq m_{s3}$, u_n can be determined by solving Eq. (1) using the numerical method.

Define the following state variables

$$\begin{cases} z_1 = x_1 \quad \dot{z}_1 = x_2 \quad z_2 = x_3 \\ \dot{z}_2 = x_4 \quad z_3 = x_5 \quad \dot{z}_3 = x_6 . \end{cases} \tag{6}$$

Eq. (3) can be written in the state-space form

$$\begin{cases} \dot{x}_1 = x_2 \\ \dot{x}_2 = \dfrac{1}{m_1}\begin{pmatrix} c_2\left(x_4 - x_2\right) + k_2\left(x_3 - x_1\right) \\ -c_1\left(x_2 - \dot{z}_r\right) - k_1\left(x_1 - z_r\right) \end{pmatrix} \\ \dot{x}_3 = x_4 \\ \dot{x}_4 = \dfrac{1}{m_2}\begin{pmatrix} c_3\left(x_6 - x_4\right) + F_{s3} - c_2\left(x_4 - x_2\right) \\ -k_2\left(x_3 - x_1\right) - U_s\left(t\right) \end{pmatrix} \\ \dot{x}_5 = x_6 \\ \dot{x}_6 = \vartheta\left(-c_3\left(x_6 - x_4\right) - F_{s3} + U_s\left(t\right)\right) \end{cases} \tag{7}$$

where $\vartheta = 1/m_3$ denotes the total mass of the vehicle seat and human body is an uncertain parameter. Assume that the extent of the uncertain parameter ϑ is known and satisfies the following relationship:

$$\vartheta \in \Omega_\vartheta = \left\{\vartheta : \vartheta_{\min} \le \vartheta \le \vartheta_{\max}\right\}, \tag{8}$$

where $\vartheta_{\min}$ and $\vartheta_{\max}$ are the lower and upper bounds of the uncertain parameter ϑ and are assumed to be known parameters. The nonlinear and linear spring forces of the vehicle seat in Eq. (7) using the state variables can be written in the general form as m_3 is an uncertain parameter:

$$\begin{cases} F_{s3} = K_v\left(1-2k\right)\left(x_5 - x_3 + u_n\right) - \left(m_3 - m_{s3}\right)g \\ \qquad +2kK_vL(1-\hat{\lambda})\dfrac{\left(x_5 - x_3 + u_n\right)}{\sqrt{L^2 - \left(x_5 - x_3 + u_n\right)^2}} \\ F_{s3} = K_v\left(x_5 - x_3 + u_n\right) - \left(m_3 - m_{s3}\right)g . \end{cases} \tag{9}$$

For the active seat suspension system, there are two main performance requirements that should be considered in the controller design: (1) The vehicle ride comfort should be improved effectively, which means the designed controller should isolate vibrations transmitted from the road to the passengers and stabilize the vertical motion of the vehicle body and passengers, although the uncertain parameter exists in the system. (2) When designing the controller, the vehicle and seat suspension strokes should be kept in a certain range to prevent the suspensions from hitting the limit block and destroying the suspension mechanisms:

$$\begin{cases} |z_2 - z_1| = |x_3 - x_1| \le z_{s1\max} \\ |z_3 - z_2| = |x_5 - x_3| \le z_{s1\max} \end{cases} \tag{10}$$

where $z_{s1\max}$, $z_{s2\max}$ are the maximum vehicle and seat suspension strokes, respectively.

4. Controller design

To improve the vehicle ride comfort and maintain the vehicle and seat suspension strokes in a certain range, the controller U_s is then designed. The constrained adaptive back-stepping controller law is presented. It is convenient to use this controller law when the nonlinearity and uncertain parameter exist in the system; this controller law is based on the BLF and can achieve a less conservatism than the classic quadratic Lyapunov function (QLF) in the controller design [22]. The constrained adaptive back-stepping controller based on BLF is composed of four main steps, which are shown as follows.

Step 1: Design the virtual control function $\alpha(t)$ as the ideal function of the vertical speed function $x_6(t)$ and denote the error function $e_6(t)$ as the difference between the actual function and the virtual control function, which can be given by

$$e_6(t) = x_6(t) - \alpha(t). \tag{11}$$

Denote the reference trajectory function $x_{5r}(t)$ as the reference trajectory of the vertical displacement function $x_5(t)$ and let the error function $e_5(t)$ as the difference between these two functions, which is given as

$$e_5(t) = x_5(t) - x_{5r}(t). \tag{12}$$

Combining Eqs. (7), (11) and (12), the derivative function of the error function $e_5(t)$ can be obtained as

$$\dot{e}_5(t) = \dot{x}_5(t) - \dot{x}_{5r}(t) = e_6(t) + \alpha(t) - \dot{x}_{5r}(t). \tag{13}$$

The main objective of this step is to design the virtual control function $\alpha(t)$ to ensure that the tracking trajectory error function $e_5(t)$ as small as possible and the seat suspension stroke is maintained in the allowed range; that is, the vertical displacement function $x_5(t)$ satisfies the following condition

$$|x_5(t)| < \delta_5, \tag{14}$$

where δ_5 is a positive constant and satisfies $\delta_5 > \varepsilon_5$. Define the following Lyapunov function

$$V_5(e_5(t)) = \frac{1}{2}\ln\frac{\Delta_5^2}{\Delta_5^2 - e_5^2(t)}, \tag{15}$$

where $\Delta_5 = \delta_5 - \varepsilon_5$. Then the derivative function of function V_5 is given as

$$\dot{V}_5(e_5(t)) = \frac{e_5(t)\dot{e}_5(t)}{\Delta_5^2 - e_5^2(t)} = \frac{e_5(t)\left(e_6(t) + \alpha(t) - \dot{x}_{5r}(t)\right)}{\Delta_5^2 - e_5^2(t)}. \tag{16}$$

If the virtual control function $\alpha(t)$ is chosen as

$$\alpha(t) = \dot{x}_{5r}(t) - r_1\left(\Delta_5^2 - e_5^2(t)\right)e_5(t), \tag{17}$$

where r_1 is a positive value. Substituting Eq. (17) into Eq. (16), the following equation can be obtained:

$$\dot{V}_5(e_5(t)) = \frac{e_5(t)e_6(t)}{\Delta_5^2 - e_5^2(t)} - r_1 e_5^2(t). \tag{18}$$

If the error function $e_6(t) = 0$, $\dot{V}_5(e_5(t)) = -r_1 e_5^2(t) \le 0$, which implies that $V_5(e_5(t)) \le V_5(e_5(0))$ and $V_5(e_5(t))$ is bounded, so $e_5(t)$ is bounded, and $\dot{e}_5(t)$ is also bounded. The second derivative function of function $V_5(e_5(t))$ is $\ddot{V}_5(e_5(t)) = -2r_1 e_5(t)\dot{e}_5(t)$, so $\ddot{V}_5(e_5(t)) = -2r_1 e_5(t)\dot{e}_5(t)$ is also bounded, $\dot{V}_5(e_5(t))$ is uniformly continuous. According to the Lyapunov-like lemma, when $t \to 0$, $\dot{V}_5(e_5(t)) \to 0$, then the tracking trajectory error function $e_5(t)$ is guaranteed to converge to zero asymptotically.

Step 2: Design a constrained adaptive back-stepping controller law for $U_s(t)$; when the uncertain parameter ϑ exists in the system, the vertical speed function $x_6(t)$ can track the virtual control function $\alpha(t)$. The derivative function of error function $e_6(t)$ can be obtained as

$$\begin{cases} \dot{e}_6(t) = \vartheta\left(-c_3\left(x_6(t) - x_4(t)\right) - F_{s3}(t) + U_s(t)\right) - \dot{\alpha}(t) \\ \quad = \vartheta G(t) - \dot{\alpha}(t) \\ G(t) = -c_3\left(x_6(t) - x_4(t)\right) - F_{s3}(t) + U_s(t). \end{cases} \tag{19}$$

Define the function $\tilde{\vartheta}(t)$ as the estimate of the uncertain parameter ϑ and let the error function $e_\vartheta(t)$ as the estimation error, which is given as

$$e_\vartheta(t) = \tilde{\vartheta}(t) - \vartheta. \tag{20}$$

Because the velocity of the error function $e_\vartheta(t)$ does not have to be restricted, define the following Lyapunov function

$$V\left(e_5(t),e_6(t),e_\vartheta(t),t\right)=V_5\left(e_5(t)\right)+\frac{1}{2}e_6^2(t)+\frac{1}{2}r_\vartheta^{-1}e_\vartheta^2(t). \tag{21}$$

Then the derivative function of function $V\left(e_5(t),e_6(t),e_\vartheta(t),t\right)$ using Eq. (17) is given as

$$\begin{aligned}\dot V\left(e_5(t),e_6(t),e_\vartheta(t),t\right)&=\frac{e_5(t)e_6(t)}{\Delta_5^2-e_5^2(t)}-r_1e_5^2(t)\\&\quad+e_6(t)\dot e_6(t)+r_\vartheta^{-1}e_\vartheta(t)\dot{\tilde\vartheta}(t)\\&=e_6(t)\left(\frac{e_5(t)}{\Delta_5^2-e_5^2(t)}+\vartheta G(t)-\dot\alpha(t)\right)\\&\quad-r_1e_5^2(t)+r_\vartheta^{-1}e_\vartheta(t)\dot{\tilde\vartheta}(t).\end{aligned} \tag{22}$$

If the control law $U_s(t)$ is chosen as

$$\begin{aligned}U_s(t)&=c_3\left(x_6(t)-x_4(t)\right)+F_{s3}(t)\\&\quad+\frac{1}{\hat\vartheta}\left(\dot\alpha(t)-r_2e_6(t)-\frac{e_5(t)}{\Delta_5^2-e_5^2(t)}\right)\end{aligned} \tag{23}$$

where r_2 is a positive value. Substituting Eq. (23) into Eq. (22), the following equation can be obtained

$$\begin{aligned}\dot V\left(e_5(t),e_6(t),e_\vartheta(t),t\right)&=-r_1e_5^2(t)-r_2e_6^2(t)\\&\quad+e_\vartheta(t)\left(r_\vartheta^{-1}\dot{\tilde\vartheta}(t)-e_6(t)G(t)\right).\end{aligned} \tag{24}$$

If the adaptive law is chosen as the projection type [26]

$$\begin{aligned}\dot{\tilde\vartheta}(t)&=proj_{\hat\vartheta}\left(r_\vartheta e_6(t)G(t)\right)\\&=\begin{cases}0 & \tilde\vartheta(t)=\vartheta_{\max}\text{ and } r_\vartheta e_6(t)G(t)>0\\0 & \tilde\vartheta(t)=\vartheta_{\min}\text{ and } r_\vartheta e_6(t)G(t)<0\\ r_\vartheta e_6(t)G(t) & \text{otherwise}\end{cases}\end{aligned} \tag{25}$$

where r_ϑ is a tunable positive value.

Substituting Eq. (25) into Eq. (24), then $\dot V\left(e_5(t),e_6(t),e_\vartheta(t),t\right)=-r_1e_5^2(t)-r_2e_6^2(t)\le 0$; this indicates that $V\left(e_5(t),e_6(t),e_\vartheta(t),t\right)\le V\left(e_5(0),e_6(0),e_\vartheta(0)\right)$ and $e_5(t)$, $e_6(t)$ and $e_\vartheta(t)$ are bounded, which implies that $\dot e_5(t)$ and $\dot e_6(t)$ are also bounded. The second derivative function of function $V\left(e_5(t),e_6(t),e_\vartheta(t),t\right)$ can be obtained as

$$\ddot V\left(e_5(t),e_6(t),e_\vartheta(t),t\right)=-2r_1e_5(t)\dot e_5(t)-2r_2e_6(t)\dot e_6(t). \tag{26}$$

So $\ddot V\left(e_5(t),e_6(t),e_\vartheta(t),t\right)$ is also bounded, $\dot V\left(e_5(t),e_6(t),e_\vartheta(t),t\right)$ is uniformly continuous. According to the Lyapunov-like lemma, when $t\to 0$, $\dot V\left(e_5(t),e_6(t),e_\vartheta(t),t\right)\to 0$, then the error functions $e_5(t)$ and $e_6(t)$ will converge to zero.

Step 3: Ensure the zero dynamics of the system is stable. The constrained adaptive back-stepping controller law is a second-order error dynamic controller law; the original system is a sixth-order system, so the zero dynamics of the system has four states. Let $e_5(t)=0$ and $\dot e_5(t)=0$, the control law $U_s(t)$ is given as

$$U_s(t)=c_3\left(x_6(t)-x_4(t)\right)+F_{s3}(t)+m_3\ddot x_{5r}(t). \tag{27}$$

Substituting Eq. (27) into Eq. (7), then the zero dynamics of the system can be obtained as

$$\begin{cases}\dot x(t)=Ax(t)+w(t)\quad x(t)=\begin{pmatrix}x_1\\x_2\\x_3\\x_4\end{pmatrix}\\ A=\begin{pmatrix}0&1&0&0\\-\frac{k_1+k_2}{m_1}&-\frac{c_1+c_2}{m_1}&\frac{k_2}{m_1}&\frac{c_2}{m_1}\\0&0&0&1\\\frac{k_2}{m_2}&\frac{c_2}{m_2}&-\frac{k_2}{m_2}&-\frac{c_2}{m_2}\end{pmatrix}\\ w(t)=\begin{pmatrix}0\\\frac{k_1}{m_1}z_r+\frac{c_1}{m_1}\dot z_r\\0\\-\frac{m_3}{m_2}\ddot x_{5r}\end{pmatrix}.\end{cases} \tag{28}$$

Define the positive function $V\left(x(t)\right)=x^T(t)Hx(t)$, where the matrix $H>0$ is a positive matrix. Then the derivative function of $V\left(x(t)\right)$ using Eq. (28) is given as

$$\begin{aligned}\dot V\left(x(t)\right)&=\dot x^T(t)Hx(t)+x^T(t)H\dot x(t)\\&=x^T(t)\left(A^TH+HA\right)x(t)+2x^T(t)Hw(t).\end{aligned} \tag{29}$$

The characteristic equation of matrix A is given as

$$\begin{aligned}\left|A-sI\right|&=s^4+\frac{c_1m_2+c_2m_1+c_2m_2}{m_1m_2}s^3+\frac{k_1m_2+k_2m_1+k_2m_2+c_1c_2}{m_1m_2}s^2\\&\quad+\frac{c_1k_2+c_2k_1}{m_1m_2}s+\frac{k_1k_2}{m_1m_2}.\end{aligned} \tag{30}$$

It can be verified that the four eigenvalues of the matrix A have negative real parts. Let $A^T H + HA = -N$, where the matrix $N > 0$ is a positive matrix.

Note $2x^T(t)Hw(t) \le x^T(t)HHx(t)/\eta + \eta w^T(t)w(t)$, where η is a tunable positive value. Then the following inequality can be obtained:

$$\dot{V}(x(t)) \le \begin{pmatrix} -x^T(t)Nx(t) + \dfrac{1}{\eta}x^T(t)HHx(t) \\ +\eta w^T(t)w(t) \end{pmatrix} \le \begin{pmatrix} \left(-\lambda_{\min}(H^{-1}N) + \dfrac{1}{\eta}\lambda_{\max}(H)\right)V(x(t)) \\ +\eta w^T(t)w(t) \end{pmatrix}. \tag{31}$$

If the matrices H, N and the tunable positive value η are chosen properly, the following inequality can be ensured

$$\lambda_{\min}(H^{-1}N) - \frac{1}{\eta}\lambda_{\max}(H) \ge h_1, \tag{32}$$

where h_1 is a positive value. Assume $\eta w^T(t)w(t) \le h_2$, then Eq. (31) can be transformed into

$$\dot{V}(x(t)) \le -h_1 V(x(t)) + h_2. \tag{33}$$

Using Eq. (33), the inequality of the positive function $V(x(t))$ can be given as

$$V(x(t)) \le \left(V(x(0)) - \frac{h_2}{h_1}\right)e^{-h_1 t} + \frac{h_2}{h_1} \le h$$
$$h = \begin{cases} V(x(0)) & V(x(0)) \ge \dfrac{h_2}{h_1} \\ 2\dfrac{h_2}{h_1} - V(x(0)) & V(x(0)) < \dfrac{h_2}{h_1} \end{cases}. \tag{34}$$

From Eq. (34), it can be verified that $V(x(t))$ is bounded. Then the following inequality can be obtained:

$$|x_i(t)| \le \sqrt{\frac{h}{\lambda_{\min}(H)}} \quad i = 1 \cdots 4. \tag{35}$$

Step 4: Select the appropriate tunable parameters to maintain the vehicle and seat suspension strokes in the allowed range. Using Eq. (35), these two constraints can be expressed as

$$\begin{cases} |z_2 - z_1| = |x_3 - x_1| \le |x_3| + |x_1| \le 2\sqrt{\dfrac{h}{\lambda_{\min}(H)}} \\ |z_3 - z_2| = |x_5 - x_3| \le |x_5| + |x_3| \le \delta_5 + \sqrt{\dfrac{h}{\lambda_{\min}(H)}} \end{cases}. \tag{36}$$

Table 1. Parameter values of the active vehicle-seat-human coupled model.

Parameter	Value	Parameter	Value
m_1	60 kg	c_1	7 Ns/m
m_2	375 kg	c_2	1425 Ns/m
m_{s3}	70 kg	c_3	830 Ns/m
$m_{3\min}$	60 kg	k_1	200000 N/m
$m_{3\max}$	80 kg	k_2	15000 N/m
K_v	31000 N/m	-	

Table 2. Controlled parameter values of the active system.

Parameter	r_9	r_1	r_2	Δ_5	δ_5
Value	0.01	100	100	0.05	0.08

If the parameters δ_5 and h are chosen to be smaller values and the positive matrix H is chosen whose eigenvalues are larger. The following inequalities can be ensured:

$$2\sqrt{\frac{h}{\lambda_{\min}(H)}} \le z_{s1\max} \qquad \delta_5 + \sqrt{\frac{h}{\lambda_{\min}(H)}} \le z_{s2\max}. \tag{37}$$

Then Eq. (10) can be guaranteed and the two constraints are satisfied.

5. Numerical simulations

The dynamic characteristics of the active vehicle-seat-human coupled model under shock excitation were studied. The parameter values of this coupled model [20, 21] used in the simulations are listed in Table 1. The maximum vehicle suspension stroke ($z_{s1\max}$) and seat suspension stroke ($z_{s2\max}$) were chosen as 0.15 m and 0.1 m, respectively. The controlled parameter values of the active system are shown in Table 2. r_9, r_1 and r_2 are positive values as can be seen in Sec. 4; r_1 and r_2 are chosen as larger values and r_9 is chosen as smaller values to guarantee the function $\dot{V}_5(e_5(t))$ and $\dot{V}(e_5(t), e_6(t), e_9(t), t)$ converges to zero faster. δ_5 and ε_5 are also positive values, and are chosen based on the condition $\delta_5 > \varepsilon_5$ and Eq. (37), as can be seen in Sec. 4.

The shock excitation is caused by a discrete irregularity on the road, such as a bump or a pothole. When the road excitation is assumed to be shock excitation, the road excitation displacement z_r can be given as

$$z_r = \begin{cases} \dfrac{A_r}{2}\left(1 - \cos\left(\dfrac{2\pi V}{l}t\right)\right) & 0 \le t \le \dfrac{l}{V} \\ 0 & t > \dfrac{l}{V} \end{cases} \tag{38}$$

Table 3. Peak acceleration value of human body, maximum vehicle suspension stroke and seat suspension stroke for passive system when $m_3 = m_{s3}$.

Parameter	$\ddot{z}_{3p}$ /(m/s^2)	$\lvert z_2 - z_1 \rvert_{max}$ /m	$\lvert z_3 - z_2 \rvert_{max}$ /m
Linear	8.4826	0.1129	0.0145
QZS $\hat{\lambda} = 0.4$	5.4666	0.1128	0.0185
QZS $\hat{\lambda} = 0.45$	5.0632	0.1128	0.0192
QZS $\hat{\lambda} = 0.5$	4.6629	0.1128	0.0199

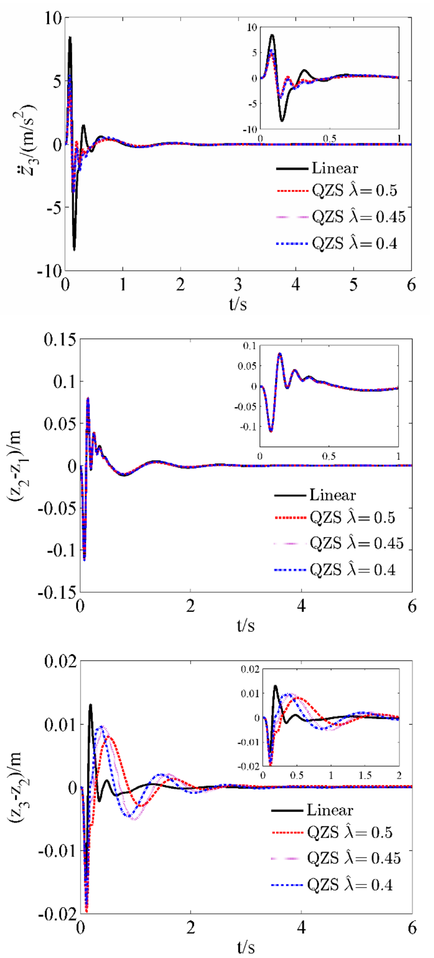

Fig. 5. Acceleration response of human body, vehicle suspension stroke and seat suspension stroke for passive system.

where A_r is the height of the bump, l is the length of the bump and V is the vehicle forward velocity. In this simulation, these parameters are chosen as $A_r = 0.1$ m, $l = 2$ m and $V = 60$ km/h.

The structural parameters of the QZS vibration isolator are chosen as $k = 1$ and $L = 0.2$ m; when the parameter $\hat{\lambda}$ takes different values, the time histories of acceleration response of human body, vehicle suspension stroke and seat suspension stroke for passive system are shown in Fig. 5. In this case, $m_3 = m_{s3} = 70$ kg, the corresponding peak acceleration value of human body, maximum vehicle suspension stroke and seat suspension stroke for passive system are shown in Table 3.

Table 4. Effect of the mass m_3 on the peak acceleration response of human body and maximum seat suspension stroke for passive system with linear seat suspension.

m_3 /kg	60	65	70	75	80
$\ddot{z}_{3p}$ /(m/s^2)	9.2133	8.8337	8.4826	8.1572	7.855
$\lvert z_3 - z_2 \rvert_{max}$ /m	0.0134	0.014	0.0145	0.015	0.0154

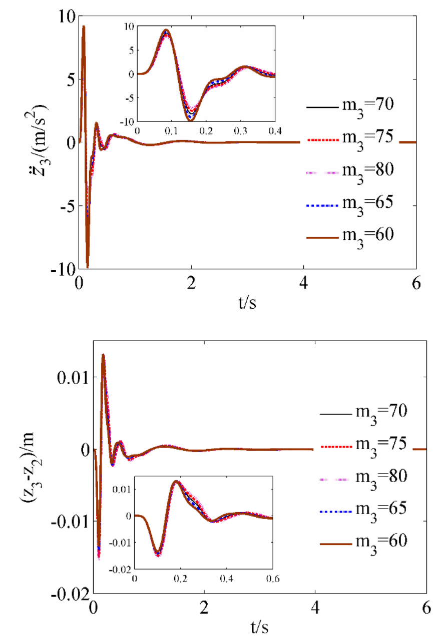

Fig. 6. Effect of the mass m_3 on the acceleration response of human body and seat suspension stroke for passive system with linear seat suspension.

It can be seen that when the QZS vibration isolator is used as seat suspension, the peak acceleration value of human body is smaller than the linear seat suspension, the vibration attenuation time becomes shorter and the vehicle ride comfort improves effectively. When $\hat{\lambda}$ increases, which indicates the dynamic stiffness of the QZS vibration isolator is smaller in the whole displacement range, the peak acceleration value of human body decreases.

The time histories of vehicle suspension stroke are almost the same for these two kinds of seat suspensions. When using QZS vibration isolator as seat suspension, the seat suspension stroke is larger, because the dynamic stiffness of the QZS vibration isolator is smaller than the stiffness of the linear seat suspension in the displacement range. When $\hat{\lambda}$ increases, the maximum seat suspension stroke increases, but remains in the allowed stroke range. In the following analysis, $\hat{\lambda} = 0.5$ was considered.

The unload and overload conditions were then considered, which means $m_3 \neq m_{s3}$. The effects of the mass m_3 on the

Table 5. Effect of the mass m_3 on the peak acceleration response of human body and maximum seat suspension stroke for passive system with QZS vibration isolator as seat suspension.

m_3 /kg	60	65	70	75	80
$\ddot{z}_{3p}$ /(m/s^2)	6.0708	5.4499	4.6629	4.7096	4.6862
$\lvert z_3 - z_2 \rvert_{\max}$ /m	0.0174	0.0185	0.0199	0.0198	0.0198

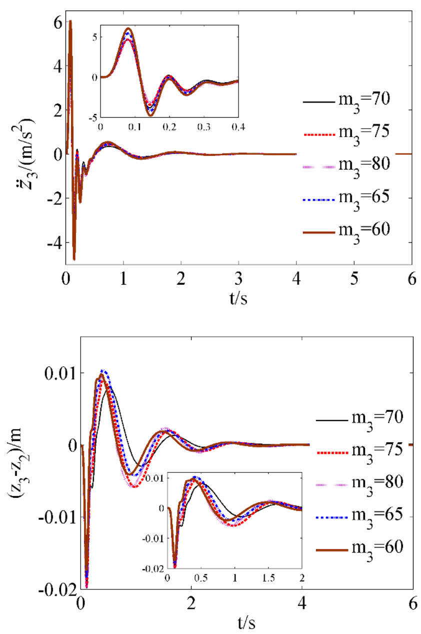

Fig. 7. Effect of the mass m_3 on the acceleration response of human body and seat suspension stroke for passive system with QZS vibration isolator as seat suspension.

acceleration response of human body and seat suspension stroke for passive system with these two kinds of seat suspensions are shown in Figs. 6 and 7, respectively. The corresponding peak acceleration value of human body and maximum seat suspension stroke for passive system with these two kinds of seat suspensions are shown in Tables 4 and 5, respectively. The vehicle suspension strokes are almost the same with different mass m_3, so it is not shown here.

When $m_3 < m_{s3}$, these two kinds of seat suspensions are in the unload condition; as the mass m_3 decreases, the peak acceleration value of human body increases while the maximum seat suspension stroke decreases. If the QZS vibration isolator is used as seat suspension, the peak acceleration value of human body increases more than the counterpart of the linear seat suspension. When $m_3 > m_{s3}$, these two kinds of seat suspension are in the overload conditions; the increase of the mass m_3 has less effect on the peak acceleration value of human body and the maximum seat suspension stroke for the QZS vibration isolator. For linear seat suspension, as the mass m_3 increases, the peak acceleration value of human body decreases while the maximum seat suspension stroke increases. In the following simulations, $m_3 = 60\,\text{kg} < m_{s3}$, the two kinds of seat suspension in the unload conditions were considered.

Table 6. Peak acceleration value of human body, maximum vehicle suspension stroke and seat suspension stroke for the active system with QZS vibration isolator as seat suspension when $x_{5r}(t) = 0$ ($m_3 = 60$).

Parameter	$\ddot{z}_{3p}$ /(m/s^2)	$\lvert z_2 - z_1 \rvert_{\max}$ /m	$\lvert z_3 - z_2 \rvert_{\max}$ /m
Linear	9.2133	0.1129	0.0134
QZS	6.0708	0.1128	0.0174
QZS+BLF	0	0.1123	0.033

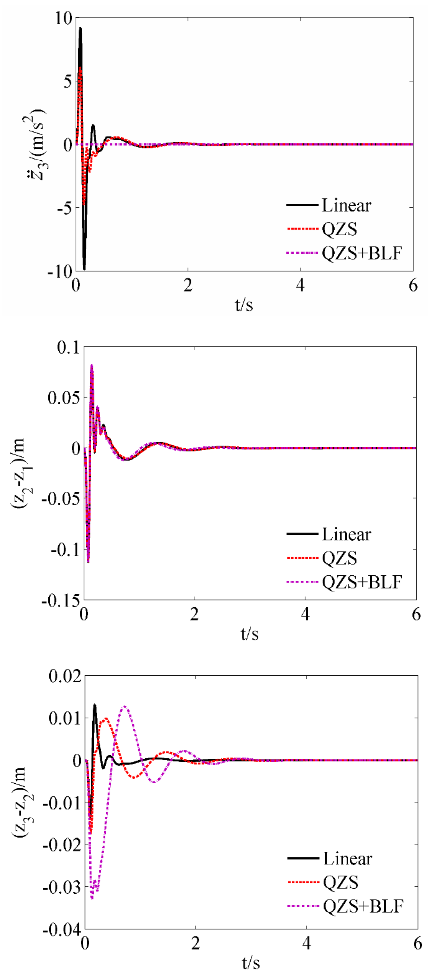

Fig. 8. Acceleration response of human body, vehicle suspension stroke and seat suspension stroke for the active system with QZS vibration isolator as seat suspension when $x_{5r}(t) = 0$ ($m_3 = 60$).

When the reference trajectory of the human body displacement($x_{5r}(t)$) is designed as $x_{5r}(t) = 0$, the acceleration response of human body, vehicle suspension stroke and seat suspension stroke for the active system with QZS vibration isolator as seat suspension are shown in Fig. 8. The corresponding curves of the passive system for these two kinds of seat suspensions are also plotted in the same figure for comparison. The corresponding peak acceleration value of human body, maximum vehicle suspension stroke and seat suspension stroke are shown in Table 6.

For the active system, when $x_{5r}(t)=0$, the acceleration response of human body is zero in the whole time domain; the vehicle ride comfort improves more effectively than the passive system, and the vehicle suspension stroke is almost the same with the passive system, while the seat suspension stroke is larger, so both the vehicle and seat suspension strokes remain in the allowed stroke range. Overall, the designed controller law can isolate the shock excitation transmitted from the road to the passengers effectively and both the vehicle and seat suspension stroke constraints are satisfied.

As can be seen in Fig. 8, when the reference trajectory $x_{5r}(t)=0$, the seat suspension stroke becomes larger although remains in the allowed stroke range. This can be improved by setting a specific designed reference trajectory in a determined time instead of the zero reference trajectory, and the determined time t_d can be changed to adjust the peak acceleration value of human body and seat suspension stroke to high or low values. The reference trajectory can be designed as a specific polynomial function, which can be given as

$$x_{5r}(t)=\begin{cases} a_0+a_1t+a_2t^2+a_3t^3+a_4t^4 & 0\le t\le t_d \\ 0 & t>t_d \end{cases} \tag{39}$$

where the coefficients a_i, $i=0\cdots 4$ are determined by the following equations:

$$\begin{cases} x_{5r}(0)=a_0=x_5(0) \quad \dot{x}_{5r}(0)=a_1=x_6(0) \\ x_{5r}(t_d)=a_0+a_1t_d+a_2t_d^2+a_3t_d^3+a_4t_d^4=0 \\ \dot{x}_{5r}(t_d)=a_1+2a_2t_d+3a_3t_d^2+4a_4t_d^3=0 \\ \ddot{x}_{5r}(t_d)=2a_2+6a_3t_d^2+4a_4t_d^3=0\,. \end{cases} \tag{40}$$

Eq. (40) can ensure that $e_5(0)=\dot{e}_5(0)=0$ and the reference trajectory $x_{5r}(t)$ is a second order differentiable function, that is, $x_{5r}(t)\in C^2$ and in the determined time t_d, $x_{5r}(t)=0$ and $\dot{x}_{5r}(t)=0$ can be guaranteed.

When the reference trajectory $x_{5r}(t)$ is designed as a specific polynomial function, the acceleration response of human body, vehicle suspension stroke, seat suspension stroke and control input force for the active system with QZS vibration isolator as seat suspension are shown in Fig. 9. In this case $x_5(0)=0.01$ m, $x_6(0)=0$. The corresponding curves of the zero reference trajectory are also plotted in the same figure for comparison. The corresponding peak acceleration value of human body, maximum vehicle suspension stroke, seat suspension stroke and control input force are shown in Table 7.

When the reference trajectory $x_{5r}(t)$ is designed as the specific polynomial function and with the increase of the determined time t_d, the peak acceleration value of human body decreases although the vibration attenuation time becomes longer. The vehicle suspension stroke is almost the same for these two different reference trajectories and changes a little when the determined time t_d takes different values. The

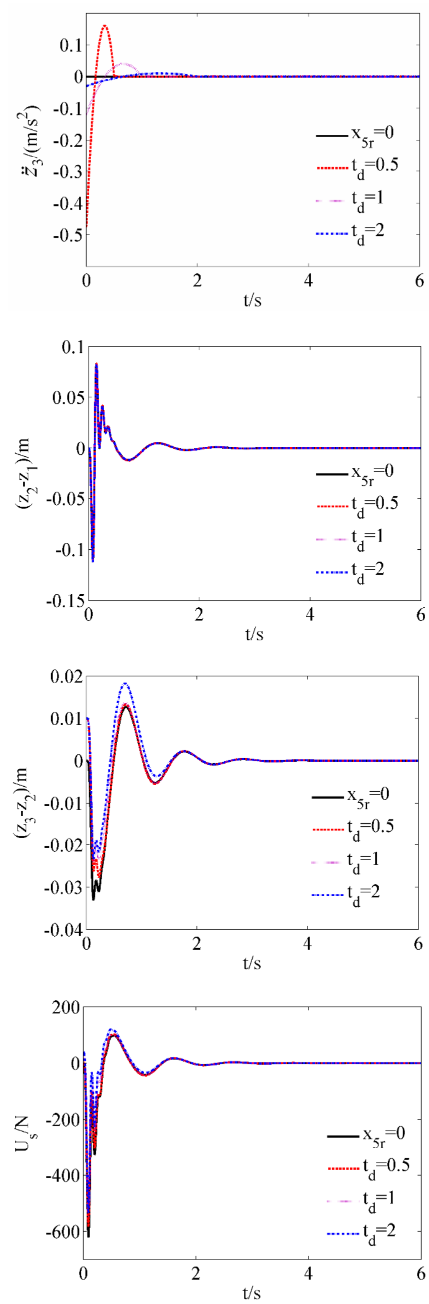

Fig. 9. Acceleration response of human body, vehicle suspension stroke, seat suspension stroke and control input force for the active system with QZS vibration isolator as seat suspension when $x_{5r}(t)\neq 0$ ($m_3=60$).

maximum seat suspension stroke and control input force are smaller than the counterparts of the zero reference trajectory and decrease as the determined time t_d increases.

6. Discussion

When the linear vibration isolator and QZS vibration isolator are used as seat suspension. respectively, it is of interest to compare the control effect of the active system with these two

Table 7. Peak acceleration value of human body, maximum vehicle suspension stroke, seat suspension stroke and control input force for the active system with QZS vibration isolator as seat suspension when $x_{5r}(t) \neq 0$ ($m_3 = 60$).

Parameter	$x_{5r} = 0$	$t_d = 0.5$s	$t_d = 1$s	$t_d = 2$s
$\ddot{z}_{3p}$ /(m/s^2)	0	0.1601	0.04	0.0101
$\lvert z_2 - z_1 \rvert_{\max}$ /m	0.1123	0.1123	0.1122	0.1123
$\lvert z_3 - z_2 \rvert_{\max}$ /m	0.033	0.0277	0.024	0.0233
$\lvert U_s \rvert_{\max}$ /N	621.035	583.614	549.011	536.856

Table 8. Peak acceleration value of human body, maximum vehicle suspension stroke, seat suspension stroke and control input force for the active system with two kinds of seat suspensions ($m_3 = 60$).

Parameter	$x_{5r} = 0$ Linear	$x_{5r} = 0$ QZS	$t_d = 1$s Linear	$t_d = 1$s QZS
$\ddot{z}_{3p}$ /(m/s^2)	0	0	0.04	0.04
$\lvert z_2 - z_1 \rvert_{\max}$ /m	0.1124	0.1123	0.1123	0.1123
$\lvert z_3 - z_2 \rvert_{\max}$ /m	0.0327	0.033	0.024	0.024
$\lvert U_s \rvert_{\max}$ /N	1204.683	621.035	938.769	549.011

kinds of seat suspensions. The comparison is clearly shown in Fig. 10. The corresponding peak acceleration value of human body, maximum vehicle suspension stroke, seat suspension stroke and control input force are shown in Table 8.

The acceleration response of the human body, vehicle suspension stroke and seat suspension stroke are almost the same for these two kinds of seat suspension when the reference trajectory $x_{5r}(t)$ is designed as two different trajectories. But the control input force is different; when using QZS vibration isolator as seat suspension, the control input force becomes much smaller.

7. Conclusion

(1) When the QZS vibration isolator is used as seat suspension for the passive system, the peak acceleration value of human body is smaller than the linear seat suspension, the vibration attenuation time becomes shorter and the vehicle ride comfort improves effectively. The changing trends of vehicle suspension stroke are almost the same as the linear seat suspension. The seat suspension stroke is larger but remains in the allowed stroke range.

(2) When these two kinds of seat suspensions are in the unload condition, as the mass m_3 decreases, the peak acceleration value of human body increases, while the maximum seat suspension stroke decreases. While in the overload condition, the increase of the mass m_3 has less effect on the peak acceleration value of the human body and the maximum seat suspension stroke for the QZS vibration isolator; for the linear

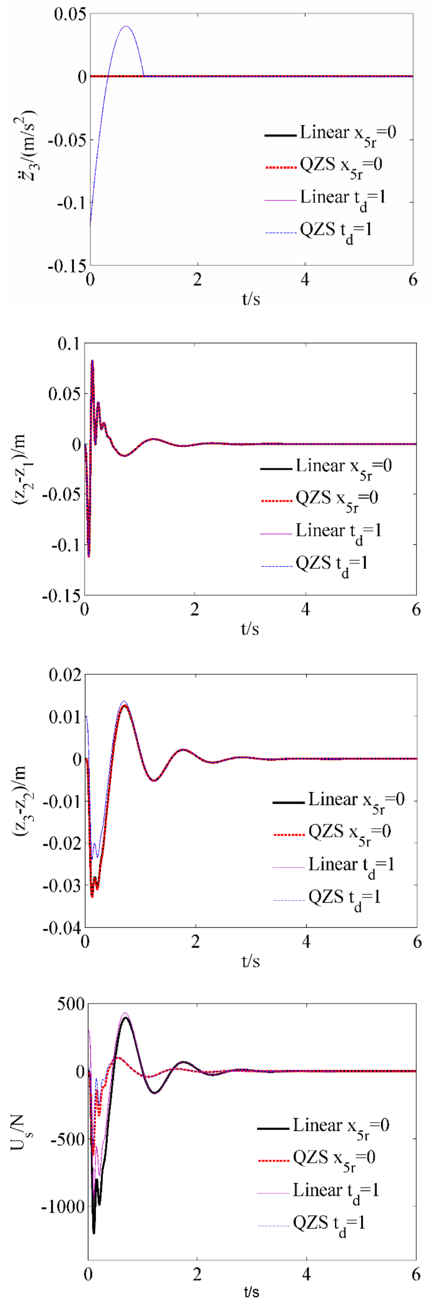

Fig. 10. Acceleration response of human body, vehicle suspension stroke, seat suspension stroke and control input force for the active system with two kinds of seat suspension ($m_3 = 60$).

seat suspension, as the mass m_3 increases, the peak acceleration value of human body decreases while the peak seat suspension stroke increases. The vehicle suspension strokes are almost the same with different mass m_3 .

(3) When the constrained adaptive back-stepping controller law based on BLF is used for the active system and the reference trajectory is designed as zero reference trajectory, the acceleration response of human body is zero in the whole time domain; the vehicle ride comfort improves more effectively than the passive system, the vehicle suspension stroke is al-

most the same with the passive system, and the seat suspension stroke is larger but remains in the allowed stroke range. The seat suspension stroke can be improved by setting the reference trajectory as the specific polynomial function, and the determined time t_d can be changed to adjust the peak acceleration value of human body and seat suspension stroke to high or low values. Then the maximum seat suspension stroke and control input force are smaller than the counterparts of the zero reference trajectory and decrease when the determined time t_d increases.

(4) When the controller law is used for these two kinds of seat suspensions, the acceleration response of human body, vehicle suspension stroke and seat suspension stroke are almost the same for the two different reference trajectories. But the control input force is different; when using QZS vibration isolator as seat suspension, the control input force becomes much smaller.

Acknowledgments

This work was supported by the National Natural Science Foundation of China (Grant Nos. 51705205 and 51675262).

References

[1] S. Rajendiran and P. Lakshmi, Simulation of PID and fuzzy logic controller for integrated seat suspension of a quarter car with driver model for different road profiles, *J. of Mechanical Science and Technology*, 30 (10) (2016) 4565-4570.

[2] P. Alabuzhev, A. Gritchin, L. Kim, G. Migirenko, V. Chon and P. Stepanov, *Vibration protecting and measuring systems with quasi-zero stiffness,* Hemisphere Publishing, New York, USA (1989).

[3] R. A. Ibrahim, Recent advances in nonlinear passive vibration isolators, *J. Sound Vib.*, 314 (3) (2008) 371-452.

[4] A. Carrella, M. J. Brennan and T. P. Waters, Static analysis of a passive vibration isolation with quasi zero-stiffness characteristic, *J. Sound Vib.*, 301 (3) (2007) 678-689.

[5] A. Carrella, M. J. Brennan and T. P. Waters, Optimization of a quasi-zero-stiffness isolator, *J. of Mechanical Science and Technology*, 21 (6) (2007) 946-949.

[6] I. Kovacic, M. J. Brennan and T. P. Waters, A study of a nonlinear vibration isolator with a quasi-zero stiffness characteristic, *J. Sound Vib.*, 315 (3) (2008) 700-711.

[7] Y. Wang, S. M. Li, S. A. Neild and J. Z. Jiang, Comparison of the dynamic performance of nonlinear one and two degree-of-freedom vibration isolators with quasi-zero stiffness, *Nonlinear Dynam.*, 88 (1) (2017) 635-654.

[8] W. S. Robertson, M. R. F. Kidner, B. S. Cazzolato and A. C. Zander, Theoretical design parameters for a quasi-zero stiffness magnetic spring for vibration isolation, *J. Sound Vib.*, 326 (1-2) (2009) 88-103.

[9] N. Zhou and K. Liu, A tunable high-static low-dynamic stiffness vibration isolator, *J. Sound Vib.*, 329 (9) (2010) 1254-1273.

[10] D. L. Xu, Q. P. Yu, J. X. Zhou and S. R. Bishop, Theoretical and experimental analyses of a nonlinear magnetic vibration isolator with quasi-zero-stiffness characteristic, *J. Sound Vib.*, 332 (14) (2013) 3377-3389.

[11] X. Liu, X. Huang and H. Hua, On the characteristics of a quasi-zero stiffness isolator using Euler buckled beam as negative stiffness corrector, *J. Sound Vib.*, 332 (14) (2013) 3359-3376.

[12] X. Huang, X. Liu and H. Hua, On the characteristics of an ultra-low frequency nonlinear isolator using sliding beam as negative stiffness, *J. of Mechanical Science and Technology*, 28 (3) (2014) 813-822.

[13] A. D. Shaw, S. A. Neild and D. J. Wagg, A nonlinear spring mechanism incorporating a bistable composite plate for vibration isolation, *J. Sound Vib.*, 332 (24) (2013) 6265-6275.

[14] H. J. Ahn, S. H. Lim and C. Park, An integrated design of quasi-zero stiffness mechanism, *J. of Mechanical Science and Technology*, 30 (3) (2016) 1071-1075.

[15] T. D. Le and K. K. Ahn, A vibration isolation system in low frequency excitation region using negative stiffness structure for vehicle seat, *J. Sound Vib.*, 330 (26) (2011) 6311-6335.

[16] T. D. Le and K. K. Ahn, Fuzzy sliding mode controller of a pneumatic active isolating system using negative stiffness structure, *J. of Mechanical Science and Technology*, 26 (12) (2012) 3873-3884.

[17] T. D. Le and K. K. Ahn, Active pneumatic vibration isolation system using negative stiffness structures for a vehicle seat, *J. Sound Vib.*, 333 (5) (2014) 1245-1268.

[18] H. P. Du, W. H. Li and N. Zhang, Integrated seat and suspension control for a quarter car with driver model, *IEEE T. Veh. Technol.*, 61 (9) (2012) 3893-3908.

[19] Y. Wang, S. M. Li and C. Cheng, Dynamic characteristics of a vehicle-seat-human coupled model with quasi-zero-stiffness isolators, *J. Vib. Shock*, 35 (15) (2016) 190-196 (in Chinese).

[20] C. Papalukopoulos and S. Natsiavas, Nonlinear biodynamics of passengers coupled with quarter car models, *J. Sound Vib.*, 304 (1) (2007) 50-71.

[21] Y. Zhao, L. Zhao and H. Gao, Vibration control of seat suspension using H∞ reliable control, *J. Vib. Control*, 16 (12) (2010) 1859-1879.

[22] W. C. Sun, H. H. Pan, Y. F. Zhang and H. Gao, Multi-objective control for uncertain nonlinear active suspension systems, *Mechatronics*, 24 (4) (2014) 318-327.

[23] K. P. Tee, S. S. Ge and E. H. Tay, Barrier Lyapunov functions for the control of output constrained nonlinear systems, *Automatica*, 45 (4) (2009) 918-927.

[24] K. P. Tee, S. S. Ge and E. H. Tay, Adaptive control of electrostatic microactuators with bidirectional drive, *IEEE Trans Control Syst Technol*, 17 (2) (2009) 340-352.

[25] Y. Wang, S. M. Li, C. Cheng and X. X. Jiang, Dynamic analysis of a high-static-low-dynamic-stiffness vibration iso-

lator with time-delayed feedback control, *Shock Vib.* (2015).
[26] B. Yao and L. Xu, Output feedback adaptive robust control of uncertain linear systems with disturbances, *J. Dyn. Syst-T ASME*, 128 (4) (2006) 938-945.

Yong Wang received the B.S. in Traffic and Transportation Engineering from Nanjing Forestry University, Nanjing, China, in 2010, and the Ph.D. in Vehicle Engineering from Nanjing University of Aeronautics and Astronautics, Nanjing, China, in 2016. He is a Lecturer at the Automotive Engineering Research Institute, Jiangsu University, Zhenjiang, China. His research interests include vehicle vibration analysis and control, nonlinear dynamics analysis and control.

Shunming Li received the Ph.D. in Mechanics from Xi'an Jiaotong University, Xi'an, China, in 1988. He is a Professor at the College of Energy and Power Engineering, Nanjing University of Aeronautics and Astronautics, Nanjing, China. His current research interests include noise and vibration analysis and control, signal processing, machine fault diagnosis, sensing and measurement technology.

Chun Cheng received the B.S. and Ph.D. in Vehicle Engineering from Nanjing University of Aeronautics and Astronautics, Nanjing, China, in 2013 and 2017. He is a Lecturer at the School of Mechatronic Engineering, Jiangsu Normal University, Xuzhou, China. His current research interests include vibration analysis and control.

Yuqing Su received the B.S. and M.S. in Vehicle Engineering from Nanjing University of Aeronautics and Astronautics, Nanjing, China, in 2013 and 2017. He is an Engineer at the Pan Asia Technical Automotive Center Co., Ltd. His research interests include vehicle dynamics analysis.